# Graphene-Starch based Electrodes for Flexible Sensing Applications

Noor Fadhilah Rahmat [a,b,c] Siti Aisyah Mohd Radzuan,[a,b] Atiqah Mohd Afdzaluddin [d] Gongtao Ding,[e] Chin Hua Chia [f] and Mohd Shaiful Sajab [a,b,*]

* *Corresponding author: mohdshaiful@ukm.edu.my*

*DOI: 10.15376/biores.21.2.2892-2905*

## GRAPHICAL ABSTRACT

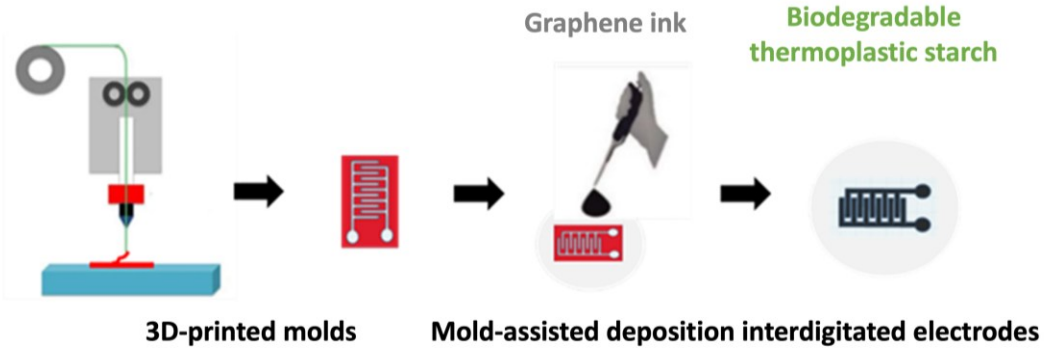

# Graphene-Starch based Electrodes for Flexible Sensing Applications

Noor Fadhilah Rahmat [a,b,c] Siti Aisyah Mohd Radzuan,[a,b] Atiqah Mohd Afdzaluddin [d] Gongtao Ding,[e] Chin Hua Chia [f] and Mohd Shaiful Sajab [a,b,*]

Flexible and sustainable electrode platforms are essential for the development of eco-friendly sensing devices. In this work, interdigitated electrodes (IDE) were fabricated *via* 3D-printed mold using graphene conductive ink on thermoplastic starch (TPS) films derived from sugar palm starch. The TPS films were prepared through solution casting with 30 wt% glycerol as a plasticizer, followed by the casting of graphene conductive ink onto the TPS substrate using 3D-printed molds with finger spacings of 1 to 3 mm. Morphological analysis revealed a well-distributed graphene layer with a thickness of 32.9 µm on the TPS film, which enhances mechanical stability and ensures high electrical conductivity. Electrochemical impedance spectroscopy (EIS) showed that the charge transfer resistance ($R_{ct}$) increased from 8.46 × $10^5$ Ω to 3.36 × $10^6$ Ω as electrode finger spacing increased from 1 mm to 3 mm which highlights the influence of gap on electron transfer. These findings confirm that biodegradable TPS substrates combined with graphene inks yield low-cost, flexible, and conductive electrodes with strong potential for electrochemical sensing applications.

*DOI: 10.15376/biores.21.2.2892-2905*

*Keywords: Graphene ink; Biodegradable electronic; Screen printed electrode; Thermoplastic starch film*

*Contact information: a: Research Center for Sustainable Process Technology (CESPRO), Faculty of Engineering and Built Environment, Universiti Kebangsaan Malaysia, 43600 Bangi, Selangor, Malaysia; b: Department of Chemical and Process Engineering, Faculty of Engineering and Built Environment, Universiti Kebangsaan Malaysia, 43600 Bangi, Selangor, Malaysia; c: Department of Physics, Centre for Defense Foundation Studies, Universiti Pertahanan Nasional Malaysia, 57000 Kuala Lumpur, Malaysia; d: Institute of Microengineering and Nanoelectronics, Universiti Kebangsaan Malaysia, 43600 UKM Bangi, Selangor, Malaysia; e: Key Laboratory of Biotechnology and Bioengineering of State Ethnic Affairs Commission, Biomedical Research Center, Northwest Minzu University, Lanzhou 730030, PR China; f: Materials Science Program, Faculty of Science and Technology, Universiti Kebangsaan Malaysia, Bangi, Malaysia; * Corresponding author: mohdshaiful@ukm.edu.my*

## INTRODUCTION

Printed electronics have emerged as a transformative technology in the development of flexible, low-cost, and scalable electronic devices. Through enabling the fabrication of high-quality electronics using techniques, such as screen-printing, gravure printing, inkjet printing, and flexographic printing, this approach addresses the growing demand for sustainable and affordable device manufacturing (Htwe *et al.* 2024). Among these, screen-printed electrodes (SPE) stand out due to their simplicity, rapid fabrication, cost-effectiveness, and scalability. The SPE are particularly valuable in electrochemical

sensing, offering portability, reproducibility, and suitability for large-scale production of disposable devices (Paimard *et al.* 2023; Crapnell and Banks 2024).

The key functional component of SPE is conductive ink, which forms the electrode pathways and dictates sensor performance. Typically composed of conductive fillers, solvents, adhesives, and functional additives, conductive inks must maintain conductivity and chemical stability during and after printing. While metals, such as silver and copper provide excellent conductivity and mechanical stability, their high cost and susceptibility to oxidation limit widespread use. Consequently, carbon-based materials, particularly graphene, have gained significant attention as alternative fillers (Aparecida *et al.* 2021; Gholamalizadeh *et al.* 2022).

Graphene, a two-dimensional nanomaterial, exhibits exceptional electrical conductivity, high electron mobility, large surface area, and superior mechanical strength, making it highly attractive for printed electronic applications (Rana *et al.* 2021; Syam Sundar *et al.* 2023; Ran *et al.* 2024). Its solution processability supports low-cost fabrication, and graphene-based inks have been widely applied in sensors and biosensors with excellent sensitivity toward analytes such as ammonia, glucose, lactose, and alcohol. These capabilities have extended graphene's impact across diverse fields, including medical diagnostics, environmental monitoring, food quality control, and system health assessment (Komeily-nia *et al.* 2021; Chia *et al.* 2022; Nan *et al.* 2022; Thakur and Kumar 2022).

A major advancement within SPE technology is the development of the interdigitated electrode (IDE), whose comb-like geometry enhances effective surface area and charge transfer, thereby improving sensitivity, selectivity, and response time. In recent years, IDE devices have emerged as a versatile electrode for portable and miniaturized sensors due to their geometry, low fabrication cost, and high sensitivity to changes in the electrical properties of the surrounding medium. IDE units enable effective impedance-based transduction by probing variations in conductivity and permittivity within a confined sensing volume and making them particularly suitable for compact and low-power sensing platforms (Sapotta *et al*. 2023). As highlighted in recent studies, the performance of IDE based sensors is strongly governed by electrode design parameters, including finger width, gap size and surface functionalization, enabling the detection of low-concentration analytes with high signal to noise ratios (Kumar *et al.* 2024).

Screen-printing further allows precise optimization of IDE parameters, while substrate selection critically influences device stability and performance. Conventional substrates, such as alumina, glass, and plastics, have been widely used but they often face limitations in conductivity and sustainability (Liang *et al.* 2021; Aleksandrova and Andreev 2022; Dokur *et al.* 2023). Recently, paper-based substrates composed of cellulose fibers have gained increasing attention as eco-friendly alternatives, offering advantages including biodegradability, mechanical flexibility, low manufacturing cost, and ease of surface modification. Owing to their porous architecture and capillary action, paper substrates can simultaneously function as mechanical supports, fluidic transport media, and sensing platforms, thereby reducing material complexity and environmental footprint in next-generation flexible electronics and sensors (Kalligosfyri and Cinti 2024).

To overcome these challenges, natural polymers, such as starch, have emerged as sustainable alternatives (Gonçalves *et al.* 2024). Starch is abundant, biodegradable, and cost-effective, and when blended with glycerol under heat and shear stress, it forms thermoplastic starch (TPS) with improved mechanical flexibility, reduced hygroscopicity, and strong intermolecular interactions (Ferreira and Andrade 2021; Rahmat *et al.* 2024a;

Stelescu *et al.* 2024). Solution-cast starch films provide smooth, uniform, and high-quality substrates with good adhesion to conductive inks, offering an eco-friendly platform for next-generation disposable electrochemical sensors (Film *et al.* 2022; Gonçalves *et al.* 2024).

In this study, TPS derived from sugar palm was developed as a sustainable substrate for printed electronics, and graphene-based conductive ink was employed to fabricate screen-printed IDE. The TPS films were prepared by solution casting with glycerol as a plasticizer, producing flexible, uniform, and biodegradable substrates. Using a 3D-printed mold, IDE patterns with varying spacings were fabricated and subsequently filled with graphene ink through a manual screen-printing process. The resulting TPS with mold-assisted graphene electrodes were systematically characterized for morphological, structural, thermal, wettability, and electrochemical properties. The tests included contact angle measurements and electrochemical impedance spectroscopy. This integrated approach has the potential not only to demonstrate the feasibility of combining natural polymer substrates with graphene-based conductive inks, but also can highlight the potential of eco-friendly printed electronics for low-cost, disposable, and scalable sensing applications. The objective of this research was to develop and evaluate eco-friendly printed interdigitated electrodes by integrating sugar palm-derived thermoplastic starch substrates with graphene-based conductive ink and to systematically investigate their structural, surface, thermal, and electrochemical properties for potential application in low-cost and scalable sensing devices.

## EXPERIMENTAL

### Materials

Thermoplastic sugar palm starch (TPS) was prepared from sugar palm collected in Jempol, Negeri Sembilan, Malaysia. Glycerol (≥ 99.0%, Sigma Aldrich, Darmstadt, Germany) served as a plasticizer, while commercial graphene conductive ink was obtained from Ugent Tech. Sdn. Bhd (Subang, Selangor, Malaysia). This commercial graphene ink contains <10 wt.% of graphene as the conductive component. It is dispersed in an organic solvent matrix primarily composed of heavy aromatic solvent naphtha (<14 w.t%) and 3,5,5-trimethylcyclohex-2-enone (>40 wt.%).

### Preparation of TPS Film

The TPS films were prepared following the procedure described in previous work (Rahmat *et al.* 2024a) with slight modifications. Briefly, 7.0 g of powdered starch was dispersed in 180 mL distilled water with glycerol at 30% w/w relative to starch. The mixture was stirred at 1000 rpm and heated at 95 °C for 50 min using a hot plate stirrer (IKA RCT basic, Staufen, Germany) to induce gelatinization. The resulting suspension was cooled, degassed under vacuum, and 20 g portions were cast into 85-mm petri dishes fitted for single-electrode fabrication. Films were dried in an oven at 45 °C overnight, peeled after 24 h, and stored under ambient conditions (25 ± 2 °C, 55 ± 1% relative humidity) prior to use.

### Fabrication of 3D-printed Mold for IDE

The IDE molds were designed using Tinkercad software (Autodesk Inc., San Rafael, CA, USA) and fabricated with a Prusa Mini 3D printer (Prusa Research, Prague,

Czech Republic) using polylactide acid (PLA) filament (1.75 mm, eSun, Shenzhen, China). The mold grooves had a depth of 100 μm and width of 150 μm, with a printing time of approximately 25 min under a nozzle diameter of 400 μm, head speed of 10 mm/s, and layer height of 1 mm. The IDE units were designed with a surface area of 10.8 mm² and a thickness of 1 mm. This process was repeated until the mold of different structures were fully fabricated with finger spacings of 1, 1.5, 2, 2.5 and 3 mm, respectively. The selection of electrode finger spacing in the range of 1 to 3 mm was guided by previous study on interdigital and coplanar electrode-based sensors. Based on this established design IDE, the 1 to 3 mm spacing was adopted in this study to enable a balanced evaluation of electrochemical performance, charge transfer behavior and fabrication reliability on flexible biopolymer substrates (Li *et al.* 2018).

For electrode fabrication, the 3D-printed PLA molds were placed onto the TPS substrates, and graphene ink (Ugent Tech. Sdn. Bhd., Subang, Selangor, Malaysia) was manually dispensed into the grooves using a syringe under controlled pressure to ensure uniform thickness and minimize defects. The process was repeated until the mold was filled after which the electrodes were air-dried at room temperature for 12 h. The IDE samples were stored in a drying box under controlled conditions at approximately 55% relative humidity (RH). This controlled storage environment was employed to minimize excessive moisture absorption and to prevent delamination or detachment of the IDE from the substrate during the storage period.

## Characterization

Morphological characterization of TPS and TPS/graphene films was performed using a field emission scanning electron microscope (FESEM; Carl Zeiss Supra 55 VP, Oberkochen, Germany). For both physical and chemical analyses, each film sample was cut into dimensions of 1 cm × 1 cm prior to measurement. Structural properties were analyzed by Fourier-transform infrared spectroscopy (FTIR) using a Nicolet 6700 FTIR spectrometer (Thermo Fisher Scientific, Waltham, MA, USA) in attenuated total reflectance (ATR) mode, with spectra collected between 4000 to 500 $cm^{-1}$ at 1 $cm^{-1}$ resolution over 42 scans. The wettability of the TPS film was evaluated using a sessile drop method with an Ossila Contact Angle Goniometer (Model L2004A1, Ossila BV, Leiden, Netherlands) equipped with a CCD digital camera, and the average of six measurements was reported. Thermal stability was investigated using simultaneous thermal analysis (STA) with a Netzsch STA 449F3 analyzer (NETZSCH-Gerätebau GmbH, Selb, Germany), which combined thermogravimetric analysis (TGA) and derivative thermogravimetry (DTG) under a nitrogen atmosphere from 30 to 800 °C at a heating rate of 10 K/min.

Electrochemical performance was assessed using electrochemical impedance spectroscopy (EIS) with a Gamry Reference 600 potentiostat (Gamry Instruments, Warminster, PA, USA). Prior to analysis, the IDE was electrically connected to the instrument by securing alligator clips onto the two circular electrode terminals and ensuring a stable and reliable electrical contact. The working and counter connections were established through these terminals, while the reference connection was configured according to the measurement setup. Once the connections were verified, the electrochemical impedance spectroscopy (EIS) measurements were performed under controlled conditions to evaluate the electrochemical behavior of the IDE.

The measurements were recorded with an AC amplitude of 100 mV across a frequency range of 100 kHz to 0.1 Hz. The impedance data were analyzed using Gamry

Echem Analyst software (Gamry Instruments, Warminster, PA, USA) and fitted to equivalent circuit models. Nyquist and Bode plots were used to evaluate charge transfer resistance, Warburg impedance, and interfacial properties at the electrode-electrolyte interface.

## RESULTS AND DISCUSSION

### Microstructural and Wettability Analysis

Figure 1 shows the different interdigitated electrode designs with finger spacings of 1, 1.5, 2, 2.5, and 3 mm. Each design incorporates two circular electrode terminals connected to an alternating arrangement of interlocking fingers. This configuration increases the effective conductive area, thereby facilitating charge transport pathways and enhancing the potential sensitivity of the electrodes. To assess the surface characteristics and structural integrity of the mold-assisted electrodes, FESEM was performed on both the TPS film substrate and the graphene ink-coated TPS film.

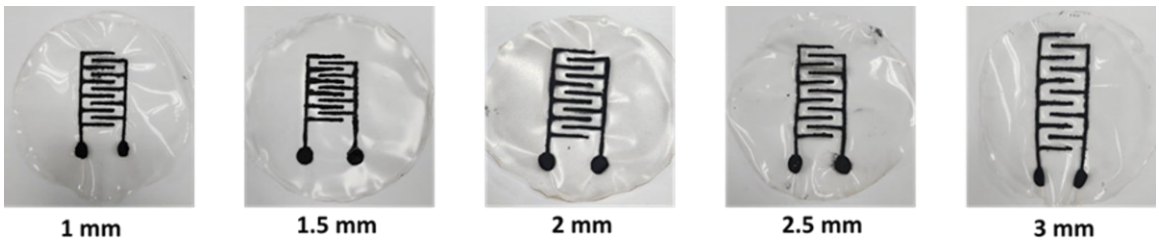


**Fig. 1.** Interdigitated electrode with different electrode finger spacing

The micrograph of the neat TPS film (Fig. 2a) reveals a relatively smooth and homogeneous surface, with no visible pores or cracks.

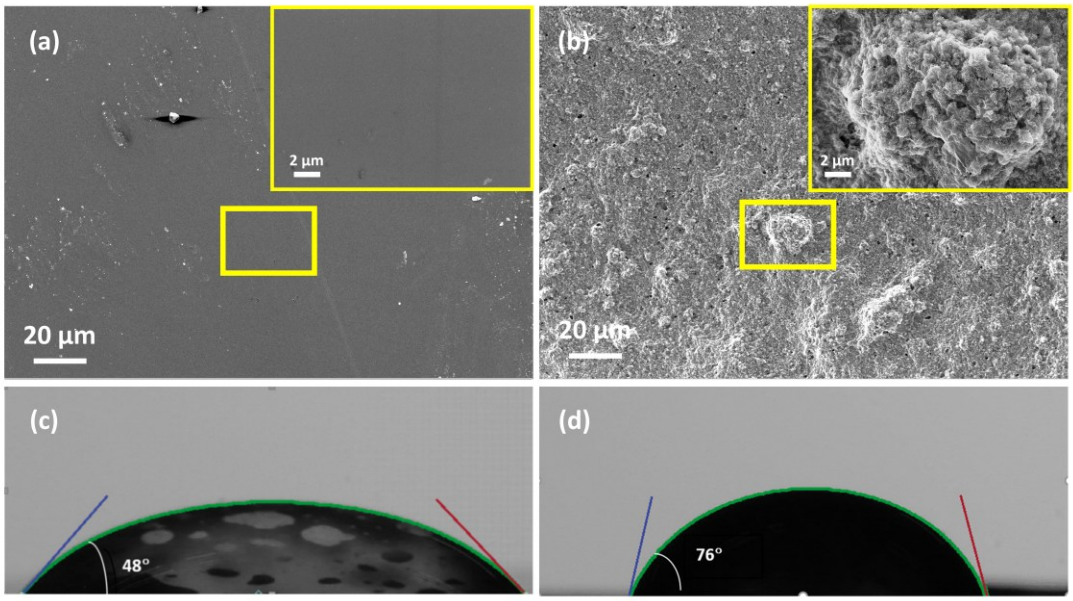


**Fig. 2.** Micrograph images of the surface (a) neat TPS film, (b) TPS-deposited graphene ink on TPS film (c) the contact angle of neat TPS film, and (d) the contact angle of graphene ink on TPS film

This morphology is attributed to the uniform dispersion of glycerol as a plasticizer within the starch matrix, which minimizes internal stresses and prevents phase separation, resulting in a compact and defect-free structure (Faisal *et al.* 2022). In contrast, the TPS film deposited with graphene ink (Fig. 2b) exhibits a rougher surface texture characterized by agglomerated graphene structures. The presence of these interconnected graphene networks indicates good deposition and adhesion of the conductive ink, while the rough morphology is advantageous for improving interfacial contact and enhancing charge transfer at the electrode surface (Rahmat *et al.* 2024b). These observations are consistent with previous studies reporting effective thermoplasticization of starch films and the rough surface of graphene-based coatings under similar processing conditions (Freitas *et al.* 2021).

The wettability of neat TPS film and TPS film integrated deposited with graphene ink was assessed using the sessile drop method, and the corresponding contact angle images are shown in Fig. 4. The neat TPS film (Fig. 2c) exhibited a water contact angle of 48°, indicating a moderately hydrophilic surface. This hydrophilicity is attributed to the abundant hydroxyl functional groups in the starch polymer chains, which readily interact with water molecules through hydrogen bonding. Such a characteristic enhances surface wettability, allowing for uniform spreading of conductive inks and promoting strong interfacial adhesion. These properties are particularly advantageous in printed electronic applications, as they contribute to reliable ink deposition and robust bonding between layers.

In contrast, the TPS film integrated with deposited graphene ink (Fig. 2d) demonstrated a significantly higher contact angle of 76°, reflecting a transition toward more hydrophobic behaviour. This change arises from the intrinsic non-polar nature of graphene sheets, which lower the surface energy of the substrate and reduce its affinity for water (Sehnal *et al.* 2024). The increase in hydrophobicity can influence the spreading behavior of subsequent liquid layers, potentially limiting ink penetration but also contributing to improved pattern definition and reduced overspreading.

The difference in contact angle between the uncoated TPS film and the graphene-deposited TPS film highlights the notable effect of surface modification on wettability. The transition from hydrophilic to moderately hydrophobic behavior suggests that the graphene coating acts as a barrier layer, altering the interfacial characteristics of the substrate. This modification has critical implications for the fabrication of printed devices, as it directly impacts ink-substrate interactions, pattern fidelity, and the overall structural stability of the printed electrodes.

## Structural and Chemical Characterization of TPS/Graphene Films

The structural properties of the TPS and TPS/graphene ink composite films were first examined using XRD, and the corresponding patterns are presented in Fig. 3(a). The neat TPS film displayed a broad diffraction peak centered around $2\theta \approx 20°$, which is characteristic of an amorphous structure (Bidari *et al.* 2023). Such a pattern is typically observed in thermoplastic starch due to the disruption of the crystalline order of starch granules upon gelatinization and plasticization with glycerol. The diffraction profile of deposited graphene ink exhibited reduced peak intensity and further broadening, suggesting that the graphene layer effectively suppressed the residual ordering within the starch network. The diminished crystallinity and broadened profile reflect enhanced structural disorder, which can be associated with strong interactions between the conductive graphene sheets and the TPS matrix. These observations are in good agreement

with previous reports demonstrating that the incorporation of graphene derivatives alters the crystalline structure of TPS. Similarly, the XRD patterns obtained in the present study exhibit changes in peak intensity and peak broadening, indicating different levels of graphene sheet dispersion within the TPS matrix (Ferreira and Andrade 2021).

To further investigate chemical interactions between the starch matrix and graphene ink, FTIR spectroscopy was performed, as shown in Fig. 3(b). For the TPS film, a broad absorbance band between 3000 to 3600 $cm^{-1}$ was observed, corresponding to O-H stretching vibrations and confirming the abundance of hydroxyl groups within the starch chains. Peaks at approximately 2920 and 2850 $cm^{-1}$ were attributed to C-H stretching vibrations, while the band near 1640 $cm^{-1}$ was assigned to O-H bending from adsorbed water, consistent with the hydrophilic nature of thermoplastic starch. A distinct absorbance around 1020 $cm^{-1}$ was observed in the fingerprint region, arising from C-O stretching vibrations of the polysaccharide ring, which is a typical feature of starch-based films (Rahmat *et al.* 2024b).

Following graphene ink deposition, noticeable changes were detected in the FTIR spectrum of the TPS/graphene ink film. The broad O-H stretching band (at 3000 to 3600 $cm^{-1}$) became less intense and broader, indicating the formation of hydrogen bonds between TPS hydroxyl groups and functional groups on the graphene. Moreover, an overall reduction in transmittance intensity across the spectrum suggested stronger intermolecular interactions and possible physical entanglement between starch chains and graphene networks. In particular, the reduction in transmittance in the 1000 to 1500 $cm^{-1}$ region can be associated with π–π stacking interactions between graphene sheets and the polysaccharide backbone, confirming successful incorporation of graphene into the TPS matrix (Ferreira and Andrade 2021). These interactions are expected to reinforce the mechanical and physicochemical stability of the film, while simultaneously enhancing electrical properties, thereby making the TPS/graphene composite a promising material platform for printed electronic and sensing applications.

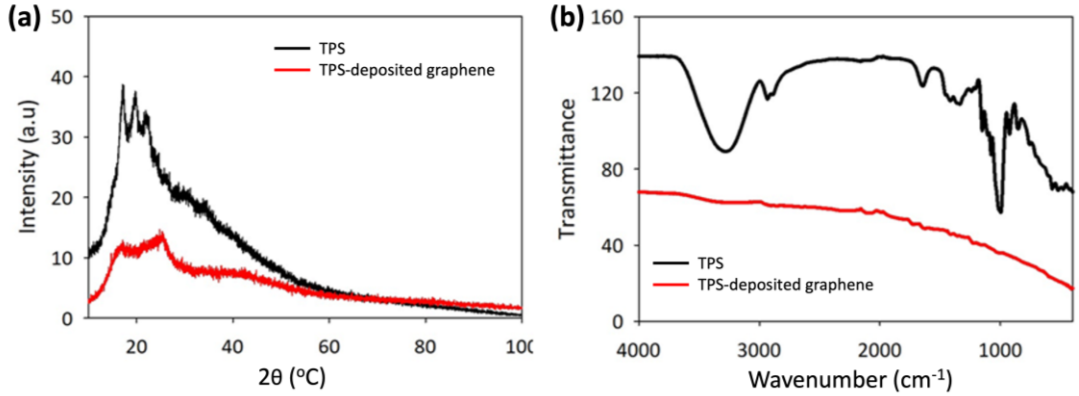


**Fig. 3.** (a) X-ray diffractometry and (b) FTIR spectrums of TPS and TPS deposited graphene ink films

## Thermal Analysis

Figure 4a shows the thermogravimetric curves of the neat TPS film and TPS-deposited graphene ink film under a controlled atmosphere. For the neat TPS film, an initial weight loss below 150 °C corresponds to the evaporation of physically absorbed moisture. This is a typical characteristic of starch-based materials because of their hygroscopic nature. The major decomposition process began at around 290 °C, with an initial mass loss

of approximately 15%, followed by a degradation step at ~340 °C, and reaching a maximum weight loss of nearly 85% at around 700 °C. These thermal decompositions are associated with the breakdown of glycosidic linkages and volatilization of small molecules such as water and carbon dioxide. The exact stability is strongly influenced by the amylose-to-amylopectin ratio, as variations in their molecular organization affect the resistance of starch to thermal degradation (Kalendova *et al.* 2021).

The TPS-deposited graphene ink film also exhibited an initial minor weight loss below 150 °C due to moisture evaporation, after which its thermal degradation profile displayed distinct deviations from the neat TPS film. A major degradation step occurred between 250 and 500 °C with a total mass loss of approximately 76%, corresponding to decomposition of the starch polymer backbone. Compared to neat TPS, the deposited graphene film displayed an earlier onset of degradation but it retained a greater residual mass beyond 700 °C. At 800 °C, the TPS-deposited graphene ink film preserved about 20% of its initial mass, which was higher than that of the TPS film. This enhancement can be attributed to the presence of graphene structures, which facilitate char formation, act as thermal barriers, and restrict the volatilization of degradation products, thereby reinforcing the composite against high-temperature decomposition (Rahmat *et al.* 2024b).

The derivative thermogravimetric curves in Fig. 4b provide further insights into the decomposition pathway. For the TPS film, the first curve below 200 °C was associated with the evaporation of absorbed water due to the hydrophilic hydroxyl groups in the starch matrix. The second, around 320 °C, corresponded to depolymerization of the starch backbone through cleavage of glycosidic bonds and the release of volatile compounds such as water and $CO_2$. At higher temperatures, further decomposition continued until the material was nearly completely decomposed. In contrast, the TPS-deposited graphene ink film exhibited a shift in the degradation peak toward lower temperatures (~260 °C) and a reduction in the maximum degradation rate. This indicates that graphene alters the thermal decomposition kinetics by modifying heat transfer and degradation pathways, ultimately leading to higher thermal stability.

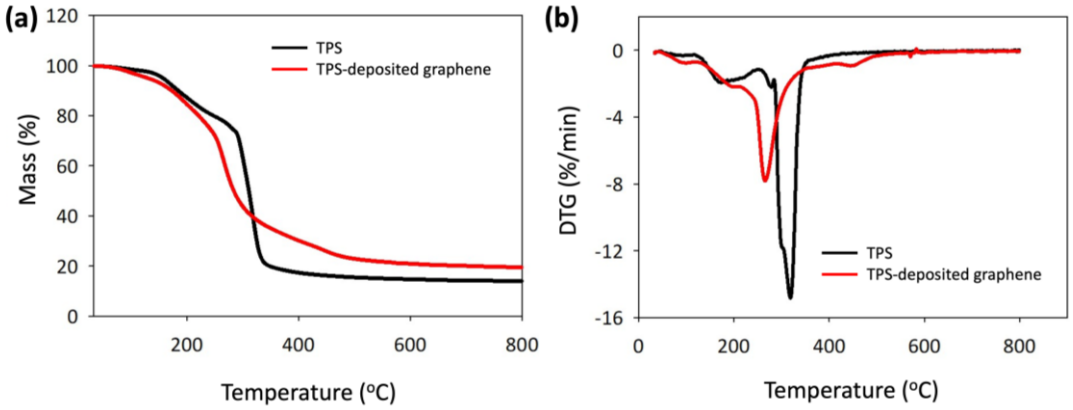


**Fig. 4.** a) TGA and (b) DTG spectrums of neat TPS and TPS-deposited graphene ink films

## Electrochemical Analysis

Electrochemical impedance spectroscopy was used to investigate the electrochemical behavior of the IDE fabricated on TPS substrates. Measurements were performed at room temperature, and the impedance spectra were fitted to an equivalent circuit model. This approach provided deeper insights into the contribution of each circuit element and its correlation with electrode structure and geometry.

The Nyquist plots of IDE with finger spacings between 1 and 3 mm (Fig. 5a) exhibited semicircular arcs characteristic of charge-transfer-limited processes. The semicircle diameter, which represents the charge transfer resistance ($R_{ct}$), increased from $8.46 \times 10^5$ Ω to $3.36 \times 10^6$ Ω as the finger spacing increased. This observation indicates that wider electrode gaps reduced the electric field intensity, thereby hindering electron transfer and raising interfacial resistance. Such behavior aligns with previous studies on gold IDEs, which also reported a positive correlation between electrode spacing and $R_{ct}$ (Mathur *et al.* 2022; Parashar and Mondal 2022). These findings indicate that the reduction in finger spacing, enhanced the electron mobility and effectively lowers the electrical resistance. Overall, the Nyquist plot analysis clearly demonstrates that reducing IDE finger spacing can be a highly effective strategy for enhancing electron mobility, lowering interfacial resistance and improving electrochemical sensitivity. This finding confirms that electrode geometry optimization is a critical design parameter for developing high-performance, flexible and sustainable electrochemical sensing platforms which suitable for detecting analytes in medical diagnostics or environmental monitoring (Patil *et al.* 2025).

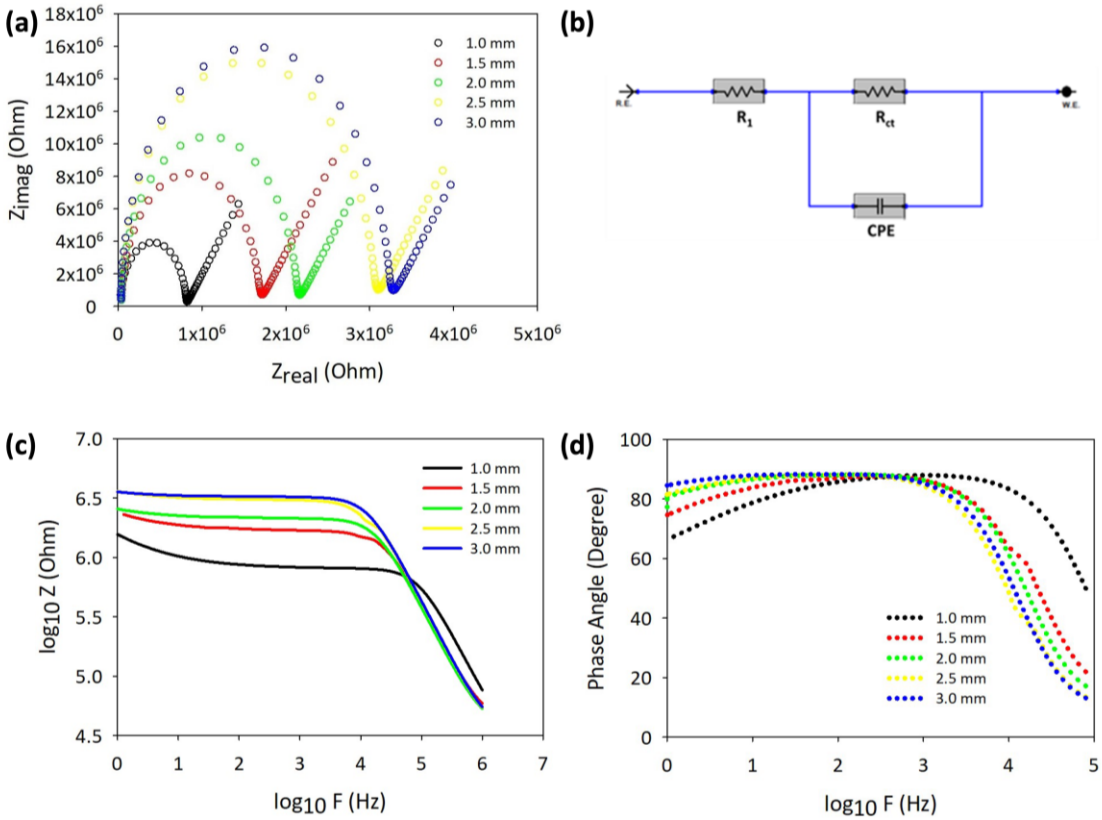


**Fig. 5.** Electrochemical impedance spectroscopy (EIS) plots: (a) Nyquist plot, (b) equivalent circuit diagram, (c) Bode plot (log Z *vs* log F) and (d) (phase angle *vs* log F)

To further interpret the impedance spectra, the data were fitted to an equivalent circuit model (Fig. 5b). The model included three primary elements: the solution resistance ($R_1$), which represents electrical contact; the charge transfer resistance ($R_{ct}$), which governs electron transport at the interface; and the double-layer capacitance ($C_{dl}$), which reflects the capacitive behavior of the electrode–electrolyte boundary. Due to surface roughness and heterogeneity, $C_{dl}$ was represented by a constant phase element (CPE) rather than an ideal capacitor. The strong agreement between the experimental and simulated curves confirms the suitability of this model for describing the interfacial processes occurring in TPS/graphene IDEs (Opančar *et al.* 2024).

The Bode plots (Fig. 5c and 5d) provided additional information on the electrode response. The impedance magnitude increased with larger finger spacing, consistent with the Nyquist data. This can be explained by the reduction of electric field concentration in wider gaps, which weakens electron transfer efficiency. Conversely, electrodes with narrower spacing generated stronger electric fields that improved sensitivity and charge transfer. The phase angle values ranged from 65° to 88°, which was slightly below the ideal 90° expected for purely capacitive systems. This deviation reflects the combined contributions of resistive and capacitive behavior at the electrode interface (Teplykh *et al.* 2024).

## CONCLUSIONS

1. Thermoplastic sugar palm starch (TPS) films were successfully prepared as biodegradable substrates, and screen-printed interdigitated electrodes (IDEs) were fabricated using graphene ink and 3D-printed molds. The combination of a smooth, defect-free TPS substrate and well-adhered graphene coating resulted in films with stable surface morphology, strong interfacial bonding, and reproducible electrode patterns.
2. Surface characterization confirmed that the addition of graphene transformed the TPS surface from hydrophilic (contact angle 48°) to more weakly hydrophilic (76°). This transition highlights the role of graphene as a surface-modifying barrier layer, altering ink spreading and adhesion behaviour.
3. The incorporation of graphene introduced strong intermolecular interactions, including hydrogen bonding and π–π stacking, confirming effective integration of graphene on the starch matrix. Thermal analysis further showed that TPS-deposited graphene ink exhibited higher residual char yield and greater thermal resistance compared to neat TPS films due to the barrier effect and char-promoting ability of graphene.
4. The electrochemical impedance spectroscopy (EIS) demonstrated that electrode geometry strongly influenced performance, with narrower finger spacing yielding lower charge transfer resistance, stronger electric field effects, and higher sensitivity. Equivalent circuit modelling confirmed the interplay of solution resistance, charge transfer resistance, and double-layer capacitance, with graphene incorporation facilitating efficient charge transport. These results underline the potential of TPS/graphene IDEs as cost-effective, flexible, and disposable electrochemical sensors, with promising applications in medical diagnostics, environmental monitoring, and sustainable electronic devices

5. This study demonstrated that biodegradable TPS substrates combined with graphene conductive ink can be successfully fabricated into flexible IDE devices with tunable electrochemical performance. The results confirm that electrode geometry plays a critical role in charge transfer behavior and validating the potential of TPS/graphene IDE as sustainable platforms for flexible sensing applications.

## ACKNOWLEDGMENTS

The authors are grateful for the support of the Universiti Kebangsaan Malaysia, Grant No. GUP-2024-063. During the preparation of this work, the authors used AI tool to improve language and readability. After using this tool, the authors have reviewed and edited the content as needed and take full responsibility for the content of the publication.

## REFERENCES CITED

Aleksandrova, M. P., and Andreev, S. K. (2022). "Design methodology and technological flow of screen-printed thick-film sensors," *IEEE Sens. J.* 22(11), 10126-10136. https://doi.org/10.1109/JSEN.2021.3093275

Aparecida, D., Araújo, G., de Oliveira, P. R., Kalinke, C., Pessoa, D., Takeuchi, R. M., Alejandro, R., Muñoz, A., Alves, J., and Campos, B. (2021). "Development of conductive inks for electrochemical sensors and biosensors," *Microchem. J.* 164, article 105998. https://doi.org/10.1016/j.microc.2021.105998

Bidari, R., Abdillah, A. A., Ponce, R. A. B., and Charles, A. L. (2023). "Characterization of biodegradable films made from taro peel (*Colocasia esculenta*) starch," *Polymers* 15(2), article 338. https://doi.org/10.3390/polym15020338

Chia, M., Ahmad, I., and Phang, S. (2022). "Starch/polyaniline biopolymer film as potential intelligent food packaging with colourimetric ammonia sensor," *Polymers* 14(6), article 1122. https://doi.org/10.3390/polym14061122

Crapnell, R. D., and Banks, C. E. (2024). "Electroanalytical overview: Screen-printed electrochemical sensing platforms," *ChemElectroChem* 11(19), article e202400370. https://doi.org/10.1002/celc.202400370

Dokur, E., Uruc, S., Kurteli, R., Gorduk, O., and Sahin, Y. (2023). "Designing disposable handmade screen-printed electrode using conductive ink for electrochemical determination of dopamine," *Ionics* 29(12), 5465-5480. https://doi.org/10.1007/s11581-023-05239-w

Faisal, M., Kou, T., Zhong, Y., and Blennow, A. (2022). "High amylose-based biocomposites: Structures, functions and applications," *Polymers* 14(6), article 1122. https://doi.org/10.3390/polym14061122

Ferreira, W. H., and Andrade, C. T. (2021). "Physical and biodegradation properties of graphene derivatives/thermoplastic starch composites," *Polysaccharides* 2(3), 582-593. https://doi.org/10.3390/polysaccharides2030035

Film, S. B., Kusumo, F., and Ngoh, G. C. (2022). "Characterization and parametric study on mechanical properties enhancement in biodegradable chitosan-reinforced films," *Polymers* 14(2), article 278. https://doi.org/10.3390/polym14020278

Freitas, P. A. V., La, C. I., Arias, F., Torres-Giner, S., and González, C. (2021). "Valorization of rice straw into cellulose microfibers for the reinforcement of

thermoplastic corn starch films," *Appl. Sci.* 11(18), article 8433. https://doi.org/10.3390/app11188433

Gholamalizadeh, N., Mazinani, S., Abdouss, M., and Mohammad, A. (2022). "Stencil printing of a highly conductive graphene ink toward flexible electrochemical biosensors for glucose monitoring," *Prog. Org. Coat.* 172, article 107083. https://doi.org/10.1016/j.porgcoat.2022.107083

Gonçalves, E. M., Silva, M., Andrade, L., and Pinheiro, J. (2024). "From fields to films: Exploring starch from agricultural raw materials for biopolymers in sustainable food packaging," *Agriculture* 14(3), article 453. https://doi.org/10.3390/agriculture14030453

Htwe, Y. Z. N., Mariatti, M., and Khan, J. (2024). "Review on solvent- and surfactant-assisted water-based conductive inks for printed flexible electronics applications," *J. Mater. Sci.- Mater. Electron.* 35, 1191-1208. https://doi.org/10.1007/s10854-024-12927-4

Kalligosfyri, P. M., and Cinti, S. (2024). "Paper-based materials for diagnostics," *ACS Materials Letters* 6(4), article 3c01474. https://doi.org/10.1021/acsmaterialslett.3c01474

Kalendova, P., Svoboda, L., Hroch, J., Honcova, P., Drobna, H., and Slang, S. (2021). "Hydrogels based on starch from various natural sources: Synthesis and characterization," *Starch/Stärke* 73(9-10), 1-13. https://doi.org/10.1002/star.202100051

Komeily-nia, Z., Qu, L., and Li, J. (2021). "Progress in the understanding and applications of the intrinsic reactivity of graphene-based materials," *Small Sci.* 1(3), article 2000026. https://doi.org/10.1002/smsc.202000026

Kumar, V., Preeti, K. M., Saini, V., Kaushik, A., and Sharma, S. K. (2024). "Interdigitated electrodes (IDEs)-supported biosensing for efficient point-of-care applications," *ECS Sensors Plus* 3(4), article ad8b59. https://doi.org/10.1149/2754-2726/ad8b59

Li, K., Wei, H., Liu, W., Meng, H., Zhang, P., and Yan, C. (2018). "3D printed stretchable capacitive sensors for highly sensitive tactile and electrochemical sensing," *Nanotechnology* 29(18), article aaafa5. https://doi.org/10.1088/1361-6528/aaafa5

Li, L., Hughes, S., Osborne, R., and Wang, X. (2024). "Printing technologies for the fabrication of ion-selective electrodes," *Sensing and Bio-Sensing Research*. 44, article 100650. https://doi.org/10.1016/j.sbsr.2024.100650

Liang, G., Feng, M., Min, J., Shin, J., Nuang, L., and Yee, W. (2021). "Potential of printed electrodes for electrochemical impedance spectroscopy (EIS): Toward membrane fouling detection," *Adv. Electron. Mater.* 7(10), article 2100043. https://doi.org/10.1002/aelm.202100043

Mathur, A., Roy, S., Nagabooshanam, S., Wadhwa, S., and Dubey, S. (2022). "Effect of gap size of gold interdigitated electrodes on the electrochemical immunosensing of cardiac troponin-I for point-of-care applications," *Sens. Actuators Rep.* 4, article 100114. https://doi.org/10.1016/j.snr.2022.100114

Nan, X., Wang, X., Kang, T., Zhang, J., Dong, L., Dong, J., and Xia, P. (2022). "Review of flexible wearable sensor devices for biomedical application," *Adv. Electron. Mater.* 8(1), article 2100738. https://doi.org/10.1002/aelm.202100043

Opančar, A., Głowacki, E. D., and Đerek, V. (2024). "Choosing the right electrode representation for modeling real bioelectronic interfaces: A comprehensive guide," *J. Neural Eng.* 21(4), article 046003. https://doi.org/10.1088/1741-2552/ad6a8b

Paimard, G., Ghasali, E., and Baeza, M. (2023). "Screen-printed electrodes: Fabrication, modification, and biosensing applications," *Chemosensors* 11(2), article 202. https://doi.org/10.3390/chemosensors11020113

Parashar, R. K., and Mondal, P. C. (2022). "The importance of electrical impedance spectroscopy and equivalent circuit analysis on nanoscale molecular electronic devices," *Adv. Funct. Mater.* 32(10), article ID 2109956. https://doi.org/10.1002/adfm.202109956

Patil, A., Kushagra, A., Amreen, K., Rao, B. P., Dubey, S. K., and Goel, S. (2025). "Enhanced electrochemical sensitivity and performance using 3D printed and screen printed interdigitated three-electrode system," *IEEE Transactions on NanoBioscience* 2025, article 3604284. https://doi.org/10.1109/TNB.2025.3604284

Rahmat, N., Sajab, M. S., Atiqah, A., Chia, C., and Ding, G. T. (2024a). "Thermoplastic sugar palm starch reinforced graphene nanoplatelets for sustainable biocomposite films," *BioResources* 19(1), 1526-1541. https://doi.org/10.15376/biores.19.1.1526-1541

Rahmat, N., Sajab, M. S., Atiqah, A., Chia, C., and Ding, G. T. (2024b). "Enhancing the electrochemical properties of biopolymer composites using starch-graphene nanoplatelets," *Polym. Compos.* 45(7), 14905-14915. https://doi.org/10.1002/pc.28809

Ran, J., Liu, Y., Feng, H., Shi, H., and Ma, Q. (2024). "A review on graphene-based electrode materials for supercapacitor," *J. Ind. Eng. Chem.* 137, 106-121. https://doi.org/10.1016/j.jiec.2024.03.043

Rana, S., Mittal, S. K., Ding, H., He, P., Wang, D., and Zha, W. (2021). "Modified screen-printed electrode using graphene ink for electrochemical sensor application," *J. Phys.- Conf. Ser*. 1912, article 012022. https://doi.org/10.1088/1742-6596/1912/1/012022

Sapotta, B., Schwotzer, M., and Franzreb, M. (2023). "Practical insights into the impedance response of interdigitated electrodes: Extraction of relative static permittivity and electrolytic conductivity," *Electroanalysis* 35(1), article e202200102. https://doi.org/10.1002/elan.202200102

Sehnal, A., Ogilvie, S. P., Clifford, K., Wood, H. J., Amorim Graf, A., Lee, F., Tripathi, M., Lynch, P. J., Large, M. J., Seyedin, S., *et al.* (2024). "Measuring the surface energy of nanosheets by emulsion inversion," *J. Phys. Chem. C* 128(40), 17073-17080. https://doi.org/10.1021/acs.jpcc.4c02893

Stelescu, M. D., Oprea, O.-C., Sonmez, M., Ficai, A., Motelica, L., Ficai, D., Georgescu, M., and Gurau, D. F. (2024). "Structural and thermal characterization of some thermoplastic starch mixtures," *Polysaccharides* 5(4), 504-522. https://doi.org/10.3390/polysaccharides5040032

Syam Sundar, L., Amin Mir, M., Waqar Ashraf, M., and Djavanroodi, F. (2023). "Synthesis and characterization of graphene and its composites for lithium-ion battery applications: A comprehensive review," *Alex. Eng. J.* 78, 224-245. https://doi.org/10.1016/j.aej.2023.07.044

Teplykh, A., Zaitsev, B., Semyonov, A., and Borodina, I. (2024). "The study of the influence of the geometry of a lateral electric field resonator on its resonant

characteristics," *Ultrasonics* 142, article 107386. https://doi.org/10.1016/j.ultras.2024.107386

Thakur, A., and Kumar, A. (2022). "Recent advances on rapid detection and remediation of environmental pollutants utilizing nanomaterials-based (bio) sensors," *Sci. Total Environ.* 834, article 155219. https://doi.org/10.1016/j.scitotenv.2022.155219

Article submitted: August 26, 2025; Peer review completed: December 20, 2025; Revised version received and accepted: January 26, 2026; Published: February 5, 2026.
DOI: 10.15376/biores.21.2.2892-2905